 CMES, vol.4, no.6, pp.619-636, 2003

A MLPG (LBIE) method for solving frequency domain elastic problems

E. J. Sellountos[1] **and D. Polyzos**[2]

Abstract: A new meshless local Petrov-Galerkin (MLPG) method for solving two dimensional frequency domain elastodynamic problems is proposed. Since the method utilizes, in its weak formulation, either the elastostatic or the frequency domain elastodynamic fundamental solution as test function, it is equivalent to the local boundary integral equation (LBIE) method. Nodal points spread over the analyzed domain are considered and the moving least squares (MLS) interpolation scheme for the approximation of the interior and boundary variables is employed. Two integral equations suitable for the integral representation of the displacement fields in the local sub- domains are used. The first utilizes the frequency domain fundamental solution, comprises only boundary integrals and exploits the elastodynamic companion solution, which is derived in the framework of the present work. The second equation makes use of the simple elastostatic fundamental solution, employs the elastostatic companion solution in order to get rid of tractions on the local boundaries and contains both boundary and volume integrals. On the global boundary, derivatives of the shape functions of the MLS approximation are avoided by considering displacements and tractions as independent variables. Direct numerical techniques for the accurate evaluation of both surface and volume integrals are employed and presented in detail. All the strongly singular integrals are computed directly through highly accurate integration techniques. Three representative numerical examples that demonstrate the accuracy of the proposed methodology are provided.

keyword: LBIE method, meshless method, frequency domain companion solution, elastodynamics

[1] Department of Mech. Engng. University of Patras (Greece), Institute of Chem. Engng. and high temperature process (Patras Greece)

[2] Department of Mech. Engng. University of Patras (Greece), Institute of Chem. Engng. and high temperature process (Patras Greece)

1 Introduction

The boundary element method (BEM) is a well-known and robust numerical tool, successfully used to date to solve various types of engineering elastic problems [Beskos (1987); Beskos (1997)]. Nevertheless, the requirement of using the fundamental solution of the differential equation or system of differential equations that describe the problem of interest renders BEM less attractive than FEM when non-linear, non-homogeneous and anisotropic elastic problems are considered. Also, the final system of linear equations taken by a BEM formulation leads to unsymmetric and full-populated matrices the numerical treatment of which is in general computationally expensive. Although some interesting works dealing with BEM solutions of anisotropic [Kogl and Gaul (2000)] and non-homogeneous [Manolis and Pavlou (2000)] have appeared in the literature, the requirement of using fundamental solutions confines the use of the BEM to linear problems only.

Recently, [Zhu, Zhang, and Atluri (1998a)] proposed a very promising meshless methodology called Local Boundary Integral Equation (LBIE) method that seems to circumvent the two aforementioned problems associated with a conventional boundary element formulation. Their methodology is characterized as meshless since a cloud of properly distributed nodal points, covering the domain of interest as well as the surrounding global boundary, is employed instead of any boundary or finite element discretization. All nodal points belong in regular sub-domains (e.g. circles for two-dimensional problems) centered at the corresponding collocation points. When non-linear elastic problems or elastic problems with body forces are considered, the displacement field at these subdomains is described through the same surface integral equation used in the conventional static elastic BEM accompanied by volume integrals coming from the non-linear terms and/or the body forces appearing in the constitutive equations. The displacements at the local and global boundaries as well as in the interior of the sub- do-

mains are usually approximated by a moving least square (MLS) scheme. Owing to regular shapes of the sub-domains, both surface and volume integrals are easily evaluated. The local nature of the sub-domains leads to a final linear system of equations the coefficient matrix of which is sparse and not full populated as in the case of the conventional BEM. As representative works on the LBIE method one can mention the papers of [Zhu, Zhang, and Atluri (1998a)], [Zhu, Zhang, and Atluri (1998b)], [Zhu, Zhang, and Atluri (1999)] and [Zhu (1999)] in linear and non linear acoustic and potential problems, the works of [Sladek, Sladek, and Atluri (2000)], [Atluri, Sladek, Sladek, and Zhu (2000)] and [Sladek, Sladek, and Keer (2003)] dealing with non- homogeneous linear elastic and elastodynamic problems, the works of [Long and Zhang (2002)], [Sladek, Sladek, and Mang (2002a)], [Sladek, Sladek, and Mang (2002b)] and [Sladek, Sladek, and Mang (2003)] for plates, the works of [Sladek, Sladek, and Atluri (2001)] and [Sladek, Sladek, and Keer (2002)] for thermoelastic and diffusion problems respectively, and the work of [Sladek and Sladek (2003)] for treating micropolar elastic problems. Details concerning the numerical implementation of the LBIE method, the representation of field variables through meshless interpolation schemes and the numerical evaluation of surface and volume integrals can be found in the works of [Atluri, Kim, and Cho (1999)], [Atluri and Zhu (2000)], [Sladek, Sladek, Atluri, and Keer (2000)], and [Sladek and Sladek (2002)]. Finally, a comprehensive presentation on the application of the LBIE method to different types of boundary value problems one can find in the very recent review paper of [Sladek, Sladek, and Atluri (2002)].

In this paper a new meshless LBIE method for solving two dimensional (2D) frequency domain elastodynamic problems is demonstrated and numerically implemented. As it is explained in the works of [Atluri and Zhu (1998)], [Atluri, Kim, and Cho (1999)], and [Atluri and Shen (2002b)] as well as in the book of [Atluri and Shen (2002a)], the LBIE method can be considered as a special case of the Meshless Local Petrov-Galerkin (MLPG) approach proposed by Atluri and co-workers. This facts explains the use of the initials MLPG (LBIE) in the title of the present work. The interior as well as the boundary of the domain of interest are covered by properly distributed nodal points each of which corresponds to a circular sub-domain where a MLS approximation scheme is applied for the meshless interpolation of the interior and boundary variables. On the global boundary, displacements and tractions are considered as independent variables. The local integral representation of displacements is accomplished with the aid of BEM-type integral equations defined on the sub- domain of each node. In the present work two local integral equations are employed for the formulation of the proposed LBIE method. The first employs the frequency domain fundamental solution and avoids the local traction fields with the aid of an elastodynamic companion solution, which is analytically derived for the needs of the present work. This integral equation leads to a truly LBIE method since only boundary integrals are involved in the final formulation of the method. On the contrary the second integral equation leads to a Local Boundary/Volume Integral Equation (LB/VIE) method since it makes use of the elastostatic fundamental solution instead of the time harmonic elastodynamic one and treats the inertia terms as body forces. The numerical evaluation of the surface and volume integrals involved in the above two formulations is accomplished with the aid of some practical and very accurate techniques presented in detail, while the direct and very accurate technique of [Guiggiani and Casalini (1987)] is employed for the numerical evaluation of the singular integrals involved in both LBIE and LB/VIE formulations

Comparing the present LBIE with those of [Sladek, Sladek, and Atluri (2000)], [Atluri, Sladek, Sladek, and Zhu (2000)] and [Sladek, Sladek, and Keer (2003)] , one can say that the proposed here LBIE appears the following new elements: a) it employs either the static or the frequency domain elastodynamic fundamental solution b) on the global boundary displacements and tractions are treated as independent variables c) the surface and volume integrals are evaluated with the aid of some practical and accurate techniques, explained in the fourth section of the present paper and d) the strongly singular and hypersingular integrals are computed directly with high accuracy.

The paper is organized as follows: in the next section the local integral formulation of the LBIE and LB/VIE is presented. The MLS approximation scheme used for the interpolation of the unknown displacements and boundary tractions is explained in section 3. Next the numerical implementation of the proposed methodology, the treatment of the essential boundary conditions and the integration techniques used for the numerical evaluation of surface, volume, regular and singular integrals are described in section 4. Finally, in section 5 three numerical

examples that illustrate the accuracy of the proposed here LBIE and LB/VIE are presented.

2 Local integral equations

In this section the two local integral equations used for the formulation of the LBIE and LB/VIE are presented. As it is mentioned in the introduction, the first local integral equation employs the 2D frequency domain elastic fundamental solution and contains only boundary integrals, while the second one comprises both boundary and volume integrals since the inertia term of the elastodynamic operator is treated as body force.

2.1 Local boundary integral equations

Consider a two-dimensional linear elastic domain V surrounded by a surface S part of which is subjected to an exterior harmonic excitation. Assuming harmonic dependence on time, the amplitude $\mathbf{u}$ of the displacement vector at $\mathbf{x}$ satisfies the differential equation [Manolis and Beskos (1988)], [Dominguez (1993)]:

$$\mu\nabla^2\mathbf{u}(\mathbf{x})+(\lambda+\mu)\nabla\nabla\cdot\mathbf{u}(\mathbf{x})+\rho\omega^2\mathbf{u}(\mathbf{x})=\mathbf{0} \tag{1}$$

where λ, μ and ρ stand for the Lame constants and the mass density, respectively, ∇ is the gradient operator and ω the excitation frequency. The boundary conditions are assumed to be

$$\begin{aligned}\mathbf{u}(\mathbf{x})&=\overline{\mathbf{u}}(\mathbf{x}),\mathbf{x}\in S_u\\ \mathbf{t}(\mathbf{x})&=\overline{\mathbf{t}}(\mathbf{x}),\mathbf{x}\in S_t\end{aligned} \tag{2}$$

with $\mathbf{t}$ denoting traction vector, $\overline{\mathbf{u}}$, $\overline{\mathbf{t}}$ represent prescribed vectors and $S_u\cup S_t\equiv S$. Considering the fundamental solution of Eq. 1 [Dominguez (1993)], [Polyzos, Tsinopoulos, and Beskos (1998)] and employing Bettis reciprocal identity, one can obtain the integral representation of the above described boundary value problem in the form

$$\begin{aligned}\alpha\mathbf{u}(\mathbf{x})+\int_S\tilde{\mathbf{t}}^*(\mathbf{x},\mathbf{y})\cdot\mathbf{u}(\mathbf{y})\,dS_y=\\ \int_S\tilde{\mathbf{u}}^*(\mathbf{x},\mathbf{y})\cdot\mathbf{t}(\mathbf{y})\,dS_y\end{aligned} \tag{3}$$

where $\tilde{\mathbf{u}}^*$, $\tilde{\mathbf{t}}^*$ are the dynamic fundamental displacement and the corresponding traction tensor, respectively, and α is the well known jump coefficient taking the value 1 for interior field points $\mathbf{x}$ and the value $1/2$ when boundary points are considered. Since both $\tilde{\mathbf{u}}^*$ and $\tilde{\mathbf{t}}^*$ become singular only when $\mathbf{y}$ approaches $\mathbf{x}$, it is easy to find one that the integral Eq. 3 can also be written in the form

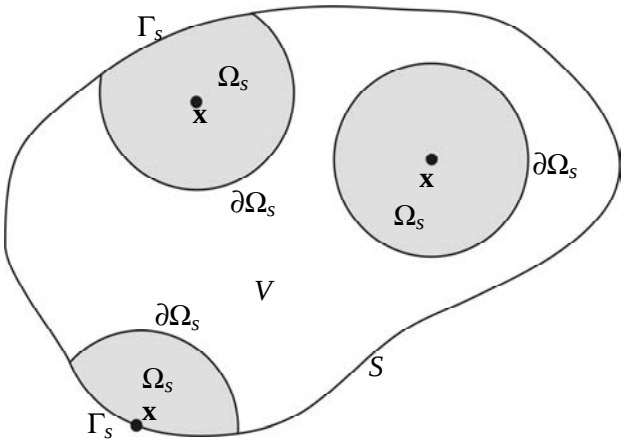

Figure 1 : Local domains and local boundaries used for the integral representation of displacements at point $\mathbf{x}$

$$\begin{aligned}\mathbf{u}(\mathbf{x})+\int_{\partial\Omega_s}\tilde{\mathbf{t}}^*(\mathbf{x},\mathbf{y})\cdot\mathbf{u}(\mathbf{y})\,dS_y=\\ \int_{\partial\Omega_s}\tilde{\mathbf{u}}^*(\mathbf{x},\mathbf{y})\cdot\mathbf{t}(\mathbf{y})\,dS_y\end{aligned} \tag{4}$$

where $\partial\Omega_s$ is the boundary of an arbitrarily small circle Ω_s centered at the field point $\mathbf{x}$. In case where the field point $\mathbf{x}$ locates either near or on the global boundary S so that the corresponding local domain Ω_s intersects the global boundary S, Eq. 4 obtains the form

$$\begin{aligned}&\alpha\mathbf{u}(\mathbf{x})+\int_{\partial\Omega_s}\tilde{\mathbf{t}}^*(\mathbf{x},\mathbf{y})\cdot\mathbf{u}(\mathbf{y})\,dS_y+\\ &\int_{\Gamma_s}\tilde{\mathbf{t}}^*(\mathbf{x},\mathbf{y})\cdot\mathbf{u}(\mathbf{y})\,dS_y=\\ &\int_{\partial\Omega_s}\tilde{\mathbf{u}}^*(\mathbf{x},\mathbf{y})\cdot\mathbf{t}(\mathbf{y})\,dS_y+\int_{\Gamma_s}\tilde{\mathbf{u}}^*(\mathbf{x},\mathbf{y})\cdot\mathbf{t}(\mathbf{y})\,dS_y\end{aligned} \tag{5}$$

with Γ_s being the part of S intersected by the sub- domain Ω_s and $\partial\Omega_s$ the boundary of Ω_s belonging in the interior space V (Fig.1). As it is explained in the work of [Atluri, Sladek, Sladek, and Zhu (2000)], the integral Eqs. 4 and 5 can be further simplified by eliminating the unknown traction vectors $\mathbf{t}$ defined on the circular boundaries $\partial\Omega_s$. This can be accomplished with the aid of a companion solution $\tilde{\mathbf{u}}^c$, which modifies the fundamental displacement $\tilde{\mathbf{u}}^*$ to be vanished on the circular boundary $\partial\Omega_s$. For the present case the companion solution is taken as solution of the boundary value problem described by

the equations

$$\begin{gathered}\mu\nabla^2\tilde{\mathbf{u}}^c(\mathbf{x},\mathbf{y})+(\lambda+\mu)\nabla\nabla\cdot\tilde{\mathbf{u}}(\mathbf{x},\mathbf{y})+\\ \rho\omega^2\tilde{\mathbf{u}}^c(\mathbf{x},\mathbf{y})=\mathbf{0}\\ \tilde{\mathbf{u}}^c(\mathbf{x},\mathbf{y})=\tilde{\mathbf{u}}^*(\mathbf{x},\mathbf{y}),\ \ \mathbf{y}\in\Omega_s\end{gathered} \tag{6}$$

and has the form

$$\tilde{\mathbf{u}}^c=\frac{1}{2\pi\mu}\left[\Psi\tilde{\mathbf{I}}-X\hat{\mathbf{r}}\otimes\hat{\mathbf{r}}\right] \tag{7}$$

where μ is the shear modulus, $\tilde{\mathbf{I}}$ is the unit tensor, $\hat{\mathbf{r}}=(\mathbf{x}-\mathbf{y})/|\mathbf{x}-\mathbf{y}|$ and $\otimes$ denotes dyadic product. The expressions of the scalar functions Ψ and X as well as the derivation of $\tilde{\mathbf{u}}^c$ can be found in Appendix A. The corresponding traction tensor $\tilde{\mathbf{t}}^c$ is written as

$$\begin{gathered}\tilde{\mathbf{t}}^c=\frac{1}{2\pi}\left[\left(\frac{d\Psi}{dr}-\frac{X}{r}\right)\left((\hat{\mathbf{r}}\cdot\hat{\mathbf{n}})\tilde{\mathbf{I}}+\hat{\mathbf{n}}\otimes\hat{\mathbf{r}}\right)-\right.\\ \frac{2}{r}X\left(\hat{\mathbf{r}}\otimes\hat{\mathbf{n}}-2\hat{\mathbf{r}}\otimes\hat{\mathbf{r}}\left(\hat{\mathbf{r}}\cdot\hat{\mathbf{n}}\right)\right)-2\frac{dX}{dr}\hat{\mathbf{r}}\otimes\hat{\mathbf{r}}\left(\hat{\mathbf{r}}\cdot\hat{\mathbf{n}}\right)+\\ \left.\left(\frac{2(1-\nu)}{1-2\nu}-2\right)\left(\frac{d\Psi}{dr}-\frac{dX}{dr}-\frac{X}{r}\right)\hat{\mathbf{r}}\otimes\hat{\mathbf{n}}\right]\end{gathered} \tag{8}$$

where $\hat{\mathbf{n}}$ is the unit vector normal to the boundary S, and ν is the Poisson's ratio. Applying Betti's reciprocal identity for the fields $\mathbf{u}$, $\tilde{\mathbf{u}}^c$ over the sub-domain Ω_s and taking into account Eq. 6, it is easy to see one that integral Eqs. 4 and 5 become

$$\mathbf{u}(\mathbf{x})+\int_{\partial\Omega_s}\left[\tilde{\mathbf{t}}^*(\mathbf{x},\mathbf{y})-\tilde{\mathbf{t}}^c(\mathbf{x},\mathbf{y})\right]\cdot\mathbf{u}(\mathbf{y})\,dS_y=\mathbf{0} \tag{9}$$

and

$$\begin{gathered}\alpha\mathbf{u}(\mathbf{x})+\int_{\partial\Omega_s\cup\Gamma_s}\left[\tilde{\mathbf{t}}^*(\mathbf{x},\mathbf{y})-\tilde{\mathbf{t}}^c(\mathbf{x},\mathbf{y})\right]\cdot\mathbf{u}(\mathbf{y})\,dS_y=\\ \int_{\Gamma_s}\left[\tilde{\mathbf{u}}^*(\mathbf{x},\mathbf{y})-\tilde{\mathbf{u}}^c(\mathbf{x},\mathbf{y})\right]\cdot\mathbf{t}(\mathbf{y})\,dS_y\end{gathered} \tag{10}$$

The boundary integral Eq. 9 describes locally the displacement field at any point $\mathbf{x}\in V\cup S$ in terms of displacements defined on the surface of the sub domain Ω_s. For points being near or on the global boundary S, the corresponding displacement fields are described by the integral Eq. 10, which contains boundary integrals defined on the circular surface $\partial\Omega_s$ as well as on the portion of the global boundary Γ_s intersected by the sub-domain Ω_s.

2.2 Local boundary/volume integral equations

An alternative to above described formulation is that of utilizing in Eq. 4 and Eq. 5 the elastostatic fundamental solution instead of the more complicated elastodynamic one. In that case, the inertia term $\rho\omega^2\mathbf{u}$ of Eq. 1 is treated as body force, thus inserting volume integrals in the form of the local integral Eqs 4 and 5, respectively, i.e.,

$$\begin{gathered}\mathbf{u}(\mathbf{x})+\int_{\partial\Omega_s}\tilde{\mathbf{T}}^*(\mathbf{x},\mathbf{y})\cdot\mathbf{u}(\mathbf{y})\,dS_y=\\ \int_{\partial\Omega_s}\tilde{\mathbf{U}}^*(\mathbf{x},\mathbf{y})\cdot\mathbf{t}(\mathbf{y})\,dS_y+\\ \rho\omega^2\int_{\Omega_s}\tilde{\mathbf{U}}^*(\mathbf{x},\mathbf{y})\cdot\mathbf{u}(\mathbf{y})\,dV_y\end{gathered} \tag{11}$$

$$\begin{gathered}\alpha\mathbf{u}(\mathbf{x})+\int_{\partial\Omega_s}\tilde{\mathbf{T}}^*(\mathbf{x},\mathbf{y})\cdot\mathbf{u}(\mathbf{y})\,dS_y+\\ \int_{\Gamma_s}\tilde{\mathbf{T}}^*(\mathbf{x},\mathbf{y})\cdot\mathbf{u}(\mathbf{y})\,dS_y=\\ \int_{\partial\Omega_s}\tilde{\mathbf{U}}^*(\mathbf{x},\mathbf{y})\cdot\mathbf{t}(\mathbf{y})\,dS_y+\\ \int_{\Gamma_s}\tilde{\mathbf{U}}^*(\mathbf{x},\mathbf{y})\cdot\mathbf{t}(\mathbf{y})\,dS_y+\\ \rho\omega^2\int_{\Omega_s}\tilde{\mathbf{U}}^*(\mathbf{x},\mathbf{y})\cdot\mathbf{u}(\mathbf{y})\,dV_y\end{gathered} \tag{12}$$

where $\tilde{\mathbf{U}}^*$ is the elastostatic fundamental displacement tensor and $\tilde{\mathbf{T}}^*$ the corresponding fundamental traction [Brebbia and Dominguez (1989)], [Polyzos, Tsinopoulos, and Beskos (1998)]. In order to get rid of the unknown tractions on the circular boundaries $\partial\Omega_s$, the elastostatic companion solution $\tilde{\mathbf{U}}^c$, derived in the work of [Atluri, Sladek, Sladek, and Zhu (2000)], is employed. This companion solution, which for illustration purposes is also derived in Appendix A, satisfies the equations

$$\begin{gathered}\mu\nabla^2\mathbf{U}^c(r)+(\lambda+\mu)\nabla\nabla\cdot\mathbf{U}^c(r)=\mathbf{0},r\le r_0\\ \mathbf{U}^c(r_0)=\mathbf{U}^*(r_0)\end{gathered} \tag{13}$$

and has the following analytic form:

$$\begin{gathered}\mathbf{U}^c(r)=\frac{1}{8\pi\mu(1-\nu)}\frac{r^2}{r_0^2}\hat{\mathbf{r}}\otimes\hat{\mathbf{r}}+\\ \frac{1}{8\pi\mu(1-\nu)}\left[\frac{5-4\nu}{2(3-4\nu)}\left(1-\frac{r^2}{r_0^2}\right)+(4\nu-3)\ln r_0\right]\tilde{\mathbf{I}}\end{gathered} \tag{14}$$

where r_0 is the radius of the circular sub-domain Ω_s and

$r = |\mathbf{r}| = |\mathbf{x}-\mathbf{y}|$. The corresponding traction field is

$$\mathbf{T}^c = \frac{1}{4\pi(1-\nu)(3-4\nu)r_0^2} \left[3\mathbf{r}\otimes\hat{\mathbf{n}} - \hat{\mathbf{n}}\otimes\mathbf{r} - (\mathbf{r}\cdot\hat{\mathbf{n}})\tilde{\mathbf{I}}\right] \quad (15)$$

By invoking Betti's reciprocal identity for the fields $\mathbf{u}$, $\tilde{\mathbf{U}}^c$ over the sub-domain Ω_s and exploiting Eq. 13, the local integral representations of Eqs 11 and 12 obtain eventually the form

$$\mathbf{u}(\mathbf{x}) + \int_{\partial\Omega_s} \left[\tilde{\mathbf{T}}^*(\mathbf{x},\mathbf{y}) - \tilde{\mathbf{T}}^c(\mathbf{x},\mathbf{y})\right]\cdot\mathbf{u}(\mathbf{y})\, dS_y = \rho\omega^2 \int_{\Omega_s} \left[\tilde{\mathbf{U}}^*(\mathbf{x},\mathbf{y}) - \tilde{\mathbf{U}}^c(\mathbf{x},\mathbf{y})\right]\cdot\mathbf{u}(\mathbf{y})\, dV_y \quad (16)$$

and

$$\alpha\mathbf{u}(\mathbf{x}) + \int_{\partial\Omega_s\cup\Gamma_s} \left[\tilde{\mathbf{T}}^*(\mathbf{x},\mathbf{y}) - \tilde{\mathbf{T}}^c(\mathbf{x},\mathbf{y})\right]\cdot\mathbf{u}(\mathbf{y})\, dS_y = \int_{\Gamma_s} \left[\tilde{\mathbf{U}}^*(\mathbf{x},\mathbf{y}) - \tilde{\mathbf{U}}^c(\mathbf{x},\mathbf{y})\right]\cdot\mathbf{t}(\mathbf{y})\, dS_y + \rho\omega^2 \int_{\Omega_s} \left[\tilde{\mathbf{U}}^*(\mathbf{x},\mathbf{y}) - \tilde{\mathbf{U}}^c(\mathbf{x},\mathbf{y})\right]\cdot\mathbf{u}(\mathbf{y})\, dV_y \quad (17)$$

Comparing the local integral Eqs 9, 10 with the just derived ones Eqs 16 and 17, one can say that the later have the advantage of employing the simple elastostatic fundamental solution and the disadvantage of containing volume integrals.

3 MLS approximation of displacements and tractions

In almost all the LBIE methodologies appearing to date in the literature, the assembly of the local integral equations valid for each nodal point $\mathbf{x}$ is accomplished with the MLS local interpolation scheme. Details on the subject one can find in the papers of [Lancaster and Salkauskas (1981)], [Belytchko, Krongauz, Organ, and Fleming (1996)] and [Atluri, Kim, and Cho (1999)]. In this section the MLS schemes used for the approximation of the displacement field $\mathbf{u}$ and the boundary tractions $\mathbf{t}$ at the neighborhood of a point $\mathbf{x}$ are explained. Consider a set of properly distributed nodal points covering the boundary and the interior space of the analyzed domain as it is shown in Fig.2. At each internal or boundary nodal point $\mathbf{x}^{(k)}$ corresponds a circular sub- domain $\hat{\Omega}^{(k)}$ of radius $r^{(k)}$ called support domain of the node $\mathbf{x}^{(k)}$. For a given internal or boundary point $\mathbf{x}$, the support subdomains $\hat{\Omega}^{(j)}$ of the adjacent nodes $\mathbf{x}^{(j)}$, $j = 1,2,...n$

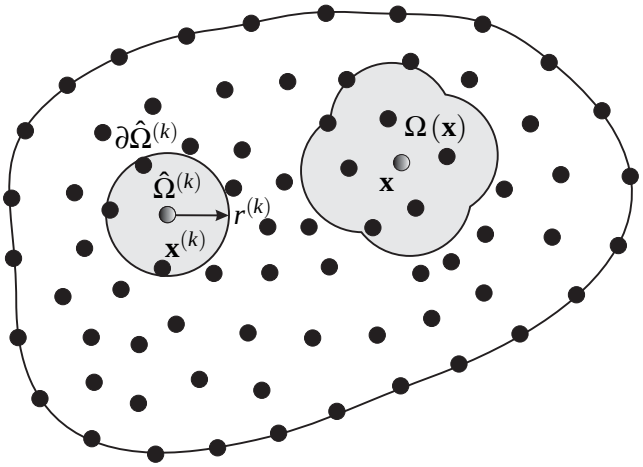

Figure 2 : Support domain $\hat{\Omega}^{(k)}$ of a node $\mathbf{x}^{(k)}$ and domain of definition $\Omega(\mathbf{x})$ used for the MLS field approximation at point $\mathbf{x}$

that contain the point $\mathbf{x}$ define a non-circular sub-domain $\Omega(\mathbf{x})$ called domain of definition of the MLS field approximation at $\mathbf{x}$. Both domains $\hat{\Omega}^{(k)}$ and $\hat{\Omega}(\mathbf{x})$ are illustrated in fig (1). The MLS approximant $u_i^h(\mathbf{x})$ of the displacement component $u_i(\mathbf{x}), i = 1$ or 2 is defined as follows

$$u_i^h(\mathbf{x}) = \mathbf{p}(\mathbf{x})\cdot\mathbf{a}^{(i)}(\mathbf{x}) \quad (18)$$

with $\mathbf{p}(\mathbf{x})$ being a vector the m components of which form a complete basis of monomials of the spatial variables x_1 and x_2, i.e.,

$$\mathbf{p}(\mathbf{x}) = [1, x_1, x_2], \ \textit{linear basis}\ (m=3) \quad (19)$$

$$\mathbf{p}(\mathbf{x}) = \left[1, x_1, x_2, x_1^2, x_1x_2, x_2^2\right], \ \textit{quadratic basis}\ (m=6) \quad (20)$$

and $\mathbf{a}^{(i)}(\mathbf{x})$ is a coefficient vector. The m unknown coefficients of $\mathbf{a}^{(i)}(\mathbf{x})$ are determined by minimizing the weighted discrete L2-norm

$$J(\mathbf{x}) = \left[\mathbf{P}\left(\mathbf{x}^{(j)}\right)\cdot\mathbf{a}^{(i)}(\mathbf{x}) - \mathbf{u}^{(i)}\left(\mathbf{x}^{(j)}\right)\right]^T \cdot \mathbf{W}(\mathbf{x})\cdot \left[\mathbf{P}\left(\mathbf{x}^{(j)}\right)\cdot\mathbf{a}^{(i)}(\mathbf{x}) - \mathbf{u}^{(i)}\left(\mathbf{x}^{(j)}\right)\right] \quad (21)$$

where $\mathbf{P}\left(\mathbf{x}^{(j)}\right)$ is a *nxm* matrix composed by the n vectors $\mathbf{p}\left(\mathbf{x}^{(j)}\right)$ of each node $\mathbf{x}^{(j)}$, $\mathbf{u}^{(i)}\left(\mathbf{x}^{(j)}\right)$ is a vector the n components of which correspond to unknown fictitious nodal displacement $u_i\left(\mathbf{x}^{(j)}\right), i = 1$ or 2 and $\mathbf{W}(\mathbf{x})$ is a diagonal Gaussian weighted matrix. In the present work

the diagonal elements of $\mathbf{W}(\mathbf{x})$ have the form (29)

$$W_{jj}(\mathbf{x}) = \left\{ \begin{array}{cc} \frac{\exp\left[-\left(\frac{d^{(j)}}{c}\right)^2\right]-\exp\left[-\left(\frac{r^{(j)}}{c}\right)^2\right]}{1-\exp\left[-\left(\frac{r^{(j)}}{c}\right)^2\right]} & d^{(j)} \le r^{(j)} \\ 0 & d^{(j)} > r^{(j)} \end{array} \right\} \tag{22}$$

where $d^{(j)} = \left|\mathbf{x}-\mathbf{x}^{(j)}\right|$ is the distance between the point $\mathbf{x}$ and the adjacent node $\mathbf{x}^{(j)}$, c is a constant controlling the shape of the weighted function W_{jj} and $r^{(j)}$ is the radius of the support domain $\hat{\Omega}^{(j)}$ where the weighted function W_{jj} is defined. The minimization of $J(\mathbf{x})$ leads to the linear relation

$$\mathbf{A}\left(\mathbf{x},\mathbf{x}^{(j)}\right)\cdot\mathbf{a}^{(j)}(\mathbf{x}) = \mathbf{B}\left(\mathbf{x},\mathbf{x}^{(j)}\right)\cdot\mathbf{u}^{(j)}\left(\mathbf{x}^{(j)}\right) \tag{23}$$

with the matrices $\mathbf{A}\left(\mathbf{x},\mathbf{x}^{(j)}\right)$, $\mathbf{B}\left(\mathbf{x},\mathbf{x}^{(j)}\right)$ having the form

$$\begin{aligned} \mathbf{A}\left(\mathbf{x},\mathbf{x}^{(j)}\right) &= \mathbf{P}^T\left(\mathbf{x}^{(j)}\right)\cdot\mathbf{W}(\mathbf{x})\cdot\mathbf{P}\left(\mathbf{x}^{(j)}\right) \\ \mathbf{B}\left(\mathbf{x},\mathbf{x}^{(j)}\right) &= \mathbf{P}^T\left(\mathbf{x}^{(j)}\right)\cdot\mathbf{W}(\mathbf{x}) \end{aligned} \tag{24}$$

Assuming properly distributed nodes $\mathbf{x}^{(j)}$ so that the inverse matrix of $\mathbf{A}\left(\mathbf{x},\mathbf{x}^{(j)}\right)$ to exist [Breitkopf, Rassineux, Touzot, and Villon (2000)], Eq. 23 yields

$$\mathbf{a}^i(\mathbf{x}) = \mathbf{A}^{-1}\left(\mathbf{x},\mathbf{x}^{(j)}\right)\cdot\mathbf{B}\left(\mathbf{x},\mathbf{x}^{(j)}\right)\cdot\mathbf{u}^{(i)}\left(\mathbf{x}^{(j)}\right) \tag{25}$$

The MLS approximant $u_i^h(\mathbf{x})$ of the component $u_i(\mathbf{x})$, $i=1$ or 2 of the displacement field $\mathbf{u}(\mathbf{x})$ is eventually obtained through a finite- element-type interpolation scheme

$$u_i^h(\mathbf{x}) = \phi\left(\mathbf{x},\mathbf{x}^{(j)}\right)\cdot\hat{\mathbf{u}}^{(j)}\left(\mathbf{x}^{(j)}\right) \tag{26}$$

where the approximation vector function $\phi\left(\mathbf{x},\mathbf{x}^{(j)}\right)$ has the form

$$\phi\left(\mathbf{x},\mathbf{x}^{(j)}\right) = \mathbf{p}(\mathbf{x})\cdot\mathbf{A}^{-1}\left(\mathbf{x},\mathbf{x}^{(j)}\right)\cdot\mathbf{B}\left(\mathbf{x},\mathbf{x}^{(j)}\right) \tag{27}$$

Thus, it is easy to see one that the MLS approximation of the displacement vector is

$$\mathbf{u}^h(\mathbf{x}) = \sum_{j=1}^{n}\phi_j\left(\mathbf{x},\mathbf{x}^{(j)}\right)\hat{\mathbf{u}}^{(j)} \tag{28}$$

where $\hat{\mathbf{u}}\left(\mathbf{x}^{(j)}\right)$ is the unknown fictitious displacement vector at the node $\mathbf{x}^{(j)}$ and

$$\phi_j\left(\mathbf{x},\mathbf{x}^{(j)}\right) = \sum_{l=1}^{m} p_l(\mathbf{x})\left[\mathbf{A}^{-1}\left(\mathbf{x},\mathbf{x}^{(j)}\right)\cdot\mathbf{B}\left(\mathbf{x},\mathbf{x}^{(j)}\right)\right]_{lj}$$

Eq. 28 represents the MLS approximation of the displacement vector at the neighborhood of an internal or boundary point $\mathbf{x}$.

The approximation of a traction vector defined at a boundary point $\mathbf{x}$ can be accomplished either by writing the traction $\mathbf{t}(\mathbf{x})$ as a combination of the adjacent nodal displacement vectors $\hat{\mathbf{u}}\left(\mathbf{x}^{(j)}\right)$ or by considering the boundary nodal traction vectors $\mathbf{t}(\mathbf{x})$ as independent variables of the problem. In the first case the traction vectors $\mathbf{t}(\mathbf{x})$ is expressed through the displacement vectors $\hat{\mathbf{u}}\left(\mathbf{x}^{(j)}\right)$ by substituting the MLS approximation (28) into the definition of tractions. More specifically, the gradient operator on Eq. 28 yields

$$\nabla_x\mathbf{u}(\mathbf{x}) = \sum_{j=1}^{n}\nabla_x\phi_j\left(\mathbf{x},\mathbf{x}^{(j)}\right)\otimes\hat{\mathbf{u}}\left(\mathbf{x}^{(j)}\right) \tag{30}$$

where the components of the vector $\nabla\phi_j$ are given by

$$\phi_{j,k} = \sum_{l=1}^{m}\left[p_{l,k}\left(\mathbf{A}^{-1}\cdot\mathbf{B}\right)_{lj} + p_l\left(\mathbf{A}^{-1}\cdot\mathbf{B}_{,k} + \mathbf{A}^{-1}_{,k}\cdot\mathbf{B}\right)_{lj}\right] \tag{31}$$

Applying Hookes law on Eq. 28 and taking into account Eq. 30 and Eq. 31, the MLS approximation of the traction vector at $\mathbf{x}$ is finally written in the form [Sladek and Sladek (2002)]

$$\mathbf{t}^h(\mathbf{x}) = \mathbf{N}(\mathbf{x})\cdot\mathbf{D}\cdot\sum_{j=1}^{n}\mathbf{E}\left(\mathbf{x},\mathbf{x}^{(j)}\right)\cdot\hat{\mathbf{u}}\left(\mathbf{x}^{(j)}\right) \tag{32}$$

where the matrix $\mathbf{N}$ contains the two components n_1, n_2 of the unit normal vector at $\mathbf{x}$, i.e.,

$$\mathbf{N}(\mathbf{x}) = \left[\begin{array}{ccc} n_1(\mathbf{x}) & 0 & n_2(\mathbf{x}) \\ 0 & n_2(\mathbf{x}) & n_1(\mathbf{x}) \end{array}\right] \tag{33}$$

and the matrices $\mathbf{D}$, $\mathbf{E}\left(\mathbf{x},\mathbf{x}^{(j)}\right)$ have the analytic form

$$\mathbf{D} = \left[\begin{array}{ccc} \lambda+2\mu & \lambda & 0 \\ \lambda & \lambda+2\mu & 0 \\ 0 & 0 & \mu \end{array}\right] \tag{34}$$

and

$$\mathbf{E}\left(\mathbf{x},\mathbf{x}^{(j)}\right) = \left[\begin{array}{cc} \phi_{j,1} & 0 \\ 0 & \phi_{j,2} \\ \phi_{j,2} & \phi_{j,1} \end{array}\right] \tag{35}$$

with $\phi_{j,1},\phi_{j,2}$ being the derivatives of Eq. 29 with respect to spatial variables x_1 and x_2, respectively, both given in the Eq. 31. In the second case where the boundary tractions are considered as independent variables of the problem, the MLS approximation of $\mathbf{t}(\mathbf{x})$ can be accomplished directly through the relation

$$\mathbf{t}^h(\mathbf{x}) = \sum_{j=1}^{n} \phi_j\left(\mathbf{x},\mathbf{x}^{(j)}\right)\hat{\mathbf{t}}\left(\mathbf{x}^{(j)}\right) \tag{36}$$

where the fictitious nodal tractions $\hat{\mathbf{t}}\left(\mathbf{x}^{(j)}\right)$ are zero for internal nodes and unknown vectors for the nodes lying on the global boundary. In other words, the approximation Eq. 36 utilizes all the nodal points belonging in the domain of definition of $\mathbf{x}$ in order to define the shape functions $\phi_j\left(\mathbf{x},\mathbf{x}^{(j)}\right)$, employs however, only the traction vectors of the adjacent boundary nodes to approximate the traction vector at $\mathbf{x}$.

In the present work, tractions and displacements are considered as independent variables and thereby Eq. 28 and Eq. 36 are employed for the MLS approximation of displacements and tractions, respectively.

4 Numerical implementation, enforcement of essential boundary conditions and evaluation of boundary and volume integrals

The subject of this section is the numerical formulation of the proposed here LBIE method and the numerical evaluation of the integrals appearing in the local integral equations described in paragraphs 2.1 and 2.2. For the sake of brevity and because of containing both surface and volume integrals only the LB/VIE method is implemented in the present section.

4.1 Numerical implementation of the LB/VIE method

Consider $N+L$ nodal points properly dispersed throughout the 2D elastic domain $V\cup S$, with L of them being distributed across the global boundary S. The support domain of each node is a circular area intersecting the corresponding support domains of the adjacent nodes. Writing the local boundary/volume integral equation Eq. 16 for the support domain corresponding to node k one obtains:

$$\begin{aligned}\mathbf{u}\left(\mathbf{x}^{(k)}\right) + \int_{\partial\hat{\Omega}_s^{(k)}} \tilde{\mathbf{T}}\left(\mathbf{x}^{(k)},\mathbf{y}\right)\cdot\mathbf{u}(\mathbf{y})\,dS_y - \\ \rho\omega^2\int_{\hat{\Omega}_s^{(k)}} \tilde{\mathbf{U}}\left(\mathbf{x}^{(k)},\mathbf{y}\right)\cdot\mathbf{u}(\mathbf{y})\,dV_y = 0\end{aligned} \tag{37}$$

where $\tilde{\mathbf{U}} = \tilde{\mathbf{U}}^* - \tilde{\mathbf{U}}^c$ and $\tilde{\mathbf{T}} = \tilde{\mathbf{T}}^* - \tilde{\mathbf{T}}^c$. Similarly, the local boundary/volume integral Eq. 17 obtains the forms

$$\begin{aligned}\alpha\mathbf{u}\left(\mathbf{x}^{(k)}\right) + \int_{\partial\hat{\Omega}_s^{(k)}} \tilde{\mathbf{T}}\left(\mathbf{x}^{(k)},\mathbf{y}\right)\cdot\mathbf{u}(\mathbf{y})\,dS_y + \\ \int_{\Gamma_s^{(k)}} \tilde{\mathbf{T}}\left(\mathbf{x}^{(k)},\mathbf{y}\right)\cdot\mathbf{u}(\mathbf{y})\,dS_y - \\ \int_{\Gamma_s^{(k)}} \tilde{\mathbf{U}}\left(\mathbf{x}^{(k)},\mathbf{y}\right)\cdot\mathbf{t}(\mathbf{y})\,dS_y - \\ \rho\omega^2\int_{\hat{\Omega}_s^{(k)}} \tilde{\mathbf{U}}\left(\mathbf{x}^{(k)},\mathbf{y}\right)\cdot\mathbf{u}(\mathbf{y})\,dV_y = 0\end{aligned} \tag{38}$$

Inserting the MLS approximations 28 and 36 for displacements and tractions respectively, into the local integral equations 37 and 38 one obtains

$$\begin{aligned}&\sum_{j=1}^{n}\phi\left(\mathbf{x}^{(k)},\mathbf{x}^{(j)}\right)\hat{\mathbf{u}}\left(\mathbf{x}^{(j)}\right) + \\ &\sum_{j=1}^{n}\left(\tilde{\mathbf{H}}^{k,j} - \tilde{\mathbf{D}}^{k,j}\right)\cdot\hat{\mathbf{u}}\left(\mathbf{x}^{(j)}\right) = 0\end{aligned} \tag{39}$$

and

$$\begin{aligned}&a\sum_{j=1}^{n}\phi\left(\mathbf{x}^{(k)},\mathbf{x}^{(j)}\right)\hat{\mathbf{u}}\left(\mathbf{x}^{(}j)\right) + \\ &\sum_{j=1}^{n}\left(\tilde{\mathbf{H}}^{k,j} - \tilde{\mathbf{D}}^{k,j} + \tilde{\mathbf{F}}^{k,j}\right)\cdot\hat{\mathbf{u}}\left(\mathbf{x}^{(j)}\right) - \\ &\sum_{j=1}^{n}\tilde{\mathbf{G}}^{k,j}\cdot\hat{\mathbf{t}}\left(\mathbf{x}^{(j)}\right) = 0\end{aligned} \tag{40}$$

where

$$\begin{aligned}\tilde{\mathbf{H}}^{k,j} &= \int_{\partial\hat{\Omega}_s^{(k)}}\tilde{\mathbf{T}}\left(\mathbf{x}^{(k)},\mathbf{y}\right)\phi_j\left(\mathbf{y},\mathbf{x}^{(j)}\right)dS_y \\ \tilde{\mathbf{F}}^{k,j} &= \int_{\Gamma_s^{(k)}}\tilde{\mathbf{T}}\left(\mathbf{x}^{(k)},\mathbf{y}\right)\phi_j\left(\mathbf{y},\mathbf{x}^{(j)}\right)dS_y \\ \tilde{\mathbf{G}}^{k,j} &= \int_{\Gamma_s^{(k)}}\tilde{\mathbf{U}}\left(\mathbf{x}^{(k)},\mathbf{y}\right)\phi_j\left(\mathbf{y},\mathbf{x}^{(j)}\right)dS_y \\ \tilde{\mathbf{D}}^{k,j} &= \rho\omega^2\int_{\hat{\Omega}_s^{(k)}}\tilde{\mathbf{U}}\left(\mathbf{x}^{(k)},\mathbf{y}\right)\phi_j\left(\mathbf{y},\mathbf{x}^{(j)}\right)dV_y\end{aligned} \tag{41}$$

The integrals $\tilde{\mathbf{H}}^{k,j}$ are always regular since $\mathbf{x}^{(k)}\notin\partial\hat{\Omega}^{(k)}$. On the contrary, the surface integrals $\tilde{\mathbf{F}}^{k,j},\tilde{\mathbf{G}}^{k,j}$ as well as the volume integrals $\tilde{\mathbf{D}}^{k,j}$ become singular when the source point $\mathbf{y}$ approaches the node $\mathbf{x}^{(k)}$. Collocating Eqs 39 and 40 at the N and L nodes distributed in V and across the boundary S, respectively, one obtains the following linear system of algebraic equations

$$\tilde{\mathbf{K}}\cdot\hat{\mathbf{u}} + \tilde{\mathbf{R}}\cdot\hat{\mathbf{t}} = 0 \tag{42}$$

where the vector $\hat{\mathbf{u}}$ comprises all the components of the fictitious displacement vectors corresponding to N internal and L boundary nodes, while the vector $\hat{\mathbf{t}}$ consists of the L fictitious boundary traction vectors. The matrices $\tilde{\mathbf{K}}$ and $\tilde{\mathbf{R}}$ contain all the $\tilde{\mathbf{H}}^{k,j}$,$\tilde{\mathbf{F}}^{k,j}$, $\tilde{\mathbf{D}}^{k,j}$ and $\tilde{\mathbf{G}}^{k,j}$ integrals, respectively, taken from the collocation of Eqs 39 and 40 at all the internal and boundary nodes.

Inserting the boundary conditions Eq. 2 in Eq. 42, with a way explained in the next paragraph, and rearranging the matrices one concludes to a final symmetric structured sparse linear system of algebraic equations written in the form

$$\tilde{\mathbf{A}} \cdot \mathbf{X} = \mathbf{b} \tag{43}$$

where the vector $\mathbf{X}$ consists of all the unknown fictitious nodal displacements and boundary tractions.

The system of equations Eq. 43 can be solved through a LU decomposition solver. Finally inserting the evaluated fictitious nodal displacements and tractions in Eqs 28 and 36, respectively, one obtains the nodal values of displacements and boundary tractions throughout the analyzed domain.

4.2 Enforcement of essential boundary conditions

The main attractive feature of the just described LB/VIE method is that all the components of the matrices $\tilde{\mathbf{K}}$, $\tilde{\mathbf{R}}$ appearing in the final system of Eq. 42 are integrals where only the MLS shape functions and not their derivatives are involved. The problem, however, is that Eq. 42 is expressed in terms of the fictitious displacements and tractions which, in general, are not identical to the corresponding nodal values due to the lack of Kronecker delta property of the MLS interpolants ϕ_j. Thus, the question here is how to enforce one the essential boundary conditions given in Eq. 2 into Eq. 42. The problem seems to be the same to that appearing in the mesh-free Galerkin methods where the final system of equations is referred to the fictitious displacements and not to the corresponding nodal ones. In those methods, the essential boundary conditions are imposed either with the aid of transformation techniques like those proposed by [Chen, Pan, Wu, and Liu (1996)], [Gunther and Liu (1998)], [Atluri, Kim, and Cho (1999)] and [Wagner and Liu (2000)] or with the use of more complicated strategies cited in the recent review paper of [Li and Liu (2002)]. Due to the nature of the proposed here LBIE method, the most suitable methods for imposing the essential boundary conditions in Eq. 42 are the simple total transformation method of [Atluri, Kim, and Cho (1999)] and the boundary transformation method proposed by Liu and co- workers. However, besides these methodologies Li and Liu report in their review paper a very interesting procedure, which enables one to enforce the essential boundary conditions directly in Eq. 42 by equating the fictitious boundary nodal values of displacements and tractions with the corresponding real ones, i.e., $\hat{\mathbf{u}}\left(\mathbf{x}^j\right) = \overline{\mathbf{u}}\left(\mathbf{x}^j\right), \mathbf{x} \in S_u$ and $\hat{\mathbf{t}}\left(\mathbf{x}^j\right) = \overline{\mathbf{t}}\left(\mathbf{x}^j\right), \mathbf{x} \in S_t$. This is possible when the boundary of the analyzed domain is piece- wise linear and the distribution of the used particles is arranged such that they are evenly distributed along the global boundary. Then, one may obtain Kronecker delta property in the MLS representation of the boundary displacements and tractions. As it is mentioned by the authors, this is a hardly known fact, which was discussed first in the paper of [Gosz and Liu (1996)]. In the present work two methodologies for the enforcement of the essential boundary conditions in Eq. 42 have been tested. The first concerns the simple transformation method of [Atluri, Kim, and Cho (1999)] where for a given map of distributed particles the MLS approximations of Eqs 28 and 36 are globally reinterpreted and expressed in terms of the nodal values of displacement and traction vectors, respectively, instead of the fictitious ones. Then, since the components of the vectors $\hat{\mathbf{u}}, \hat{\mathbf{t}}$ in Eq. 42 represent nodal and not fictitious values, the enforcement of the essential boundary conditions is straightforward. The second strategy tested in the present work is the direct procedure of [Gosz and Liu (1996)] where evenly distributed points along to the global boundary are considered and the essential boundary conditions are directly imposed on the fictitious values of displacements and tractions of Eq. 42. Although Gosz and Liu claim that this procedure works only for piece- wise linear global boundaries, numerical experiments performed in the framework of the present work shown that a Kronecker delta behavior of the MLS approximation of boundary displacements and tractions is also possible for problems with curved boundaries.

4.3 Numerical Evaluation of boundary and volume integrals

It is well known that the accuracy of the above described LBIE methodology depends on the accurate numerical evaluation of the singular and non- singular integrals appearing in the expressions of Eq. 41. Numerical experi-

ments performed in the work of [Atluri, Kim, and Cho (1999)] as well as by the authors of the present work have shown that the division of the domain of integration into small segments give much better accuracy than in the case where the integration is performed over the entire domain with a large number of integration points. Thus, the numerical evaluation of the non-singular $\mathbf{H}^{k,j}$ integrals is accomplished by dividing the boundary $\partial\hat{\Omega}_s^{(k)}$ into segments each of which is defined by the intersection of $\partial\hat{\Omega}_s^{(k)}$ with the support sub-domains of the adjustment nodes $\mathbf{x}^{(j)}$ (Fig 3(a)). Assuming that the boundary $\partial\hat{\Omega}_s^{(k)}$ is divided into M totally segments, the integral can be written as follows:

$$\mathbf{H}^{k,j} = \int_{\partial\Omega_s^{(k)}} \mathbf{T}\left(\mathbf{x}^{(k)},\mathbf{y}\right)\phi^j\, dS_y = \sum_{m=1}^{M}\int_{C_m^{(k)}} \mathbf{T}\left(\mathbf{x}^{(k)},\mathbf{y}\right)\phi^j\, dS_y \tag{44}$$

where $C_1^{(k)}\cup C_2^{(k)}\cup\ldots\cup C_M^{(k)}\equiv\partial\Omega_s^{(k)}$. Considering a polar co-ordinate system having its center at the node $\mathbf{x}^{(k)}$ and transforming to the new co-ordinates one obtains

$$\mathbf{H}^{k,j} = \sum_{m=1}^{M}\int_{\phi_1^{(m)}}^{\phi_2^{(m)}} \mathbf{T}\left(\mathbf{x}^{(k)},\mathbf{y}\right)\phi^j J_\phi\, d\phi \tag{45}$$

with $\phi_1^{(m)},\phi_2^{(m)}$ being the two polar angles define the segment $C_m^{(k)}$ and J_ϕ the Jacobian of the transformation. Applying the linear transformation $\phi = \frac{\phi_1^{(m)}+\phi_2^{(m)}}{2} + \frac{\phi_2^{(m)}-\phi_1^{(m)}}{2}\xi$ for each segment, the integral (45) is eventually written in the form

$$\mathbf{H}^{k,j} = \sum_{m=1}^{M}\int_{-1}^{1} \mathbf{T}\left(\mathbf{x}^{(k)},\mathbf{y}\right)\phi^j J_\phi J_\xi\, d\xi \tag{46}$$

and it is numerically evaluated through standard Gaussian quadrature. Similarly, for the evaluation of $\mathbf{F}^{k,j}$ and $\mathbf{G}^{k,j}$ integrals the intersected global boundary $\Gamma_s^{(k)}$ is divided into segments as it is illustrated in Fig 3(b). Utilizing for the description of the segments the space variables $z_1^{(m)}$, $z_2^{(m)}$ instead of the polar angles $\phi_1^{(m)}$, $\phi_2^{(m)}$ and applying the above-described integration procedure, the integrals of $\mathbf{F}^{k,j}$ and $\mathbf{G}^{k,j}$ are easily evaluated. When the node $\mathbf{x}^{(k)}$ lies on the global boundary S, both integrals $\mathbf{F}^{k,j}$ and $\mathbf{G}^{k,j}$ defined on the segment of containing the node $\mathbf{x}^{(k)}$ (Fig. 3(c)) become singular. In that case, the direct technique of [Guiggiani and Casalini (1987)] is employed and the integrals $\mathbf{F}^{k,j}$ and $\mathbf{G}^{k,j}$ are evaluated with high accuracy. Finally, the volume integrals $\mathbf{D}^{k,j}$ can be written in the form [Atluri, Kim, and Cho (1999)]

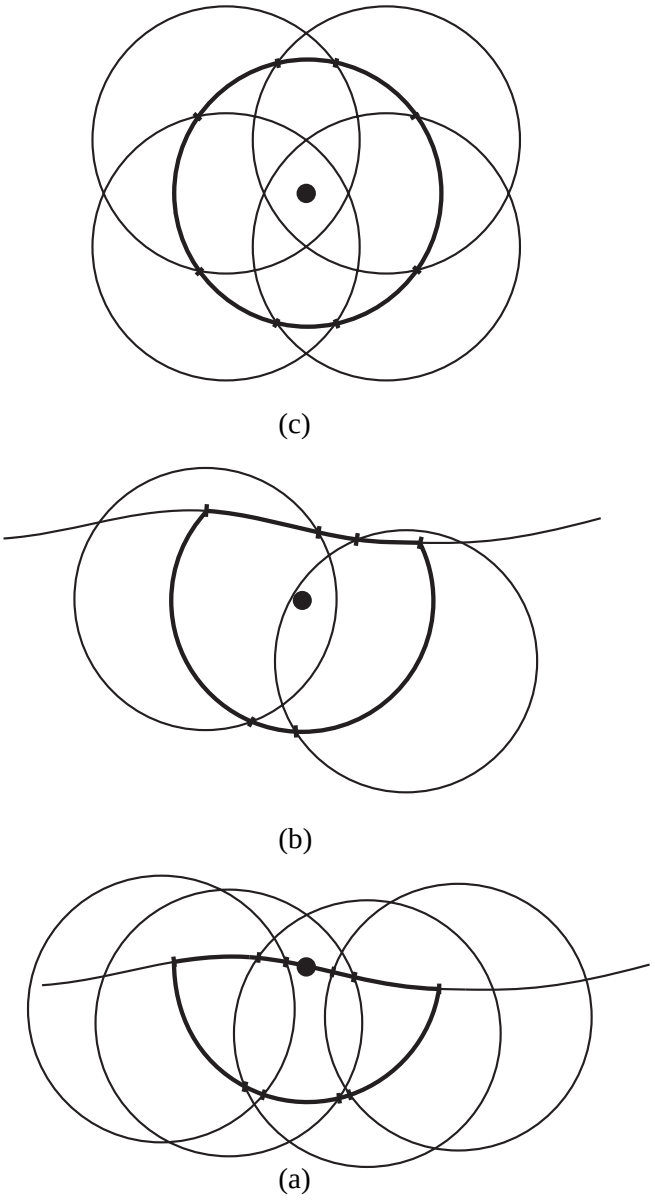

Figure 3 : Splitting of integration domains into segments when the support domain of the nodal point $\mathbf{x}^{(k)}$ (a) is entirely interior to V, (b) intersects the global boundary S and $\mathbf{x}^{(k)}$ is internal node, (c) intersects the global boundary and $\mathbf{x}^{(k)}$ is a boundary node

$$\mathbf{D}^{k,j} = \rho\omega^2\int_{\hat{\Omega}_s^{(k)}} \mathbf{U}\left(\mathbf{x}^{(k)},\mathbf{y}\right)\phi^j\, dV_y = \rho\omega^2\sum_{j=1}^{n}\int_{A^{k,j}} \mathbf{U}\left(\mathbf{x}^{(k)},\mathbf{y}\right)\phi_j\, dV_y \tag{47}$$

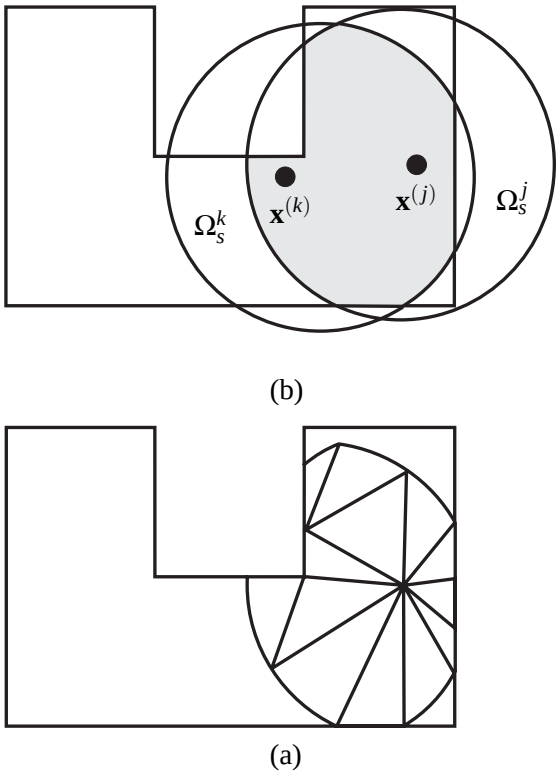

Figure 4 : (a) The integration area $A^{k,j}$ defined by the intersection of the support domains Ω_s^k,Ω_s^j with the global boundary S (b) splitting of $A^{k,j}$ into triangular segments

where $A^{k,j}$ represents the domain $\hat{\Omega}_S^{(k)} \cap \hat{\Omega}_S^{(j)}$ defined by the intersected support domains $\hat{\Omega}_S^{(k)}$ and $\hat{\Omega}_S^{(j)}$ of the nodal point $\mathbf{x}^{(k)}$ and the adjustment node $\mathbf{x}^{(j)}$, respectively. In case where the two sub-domains $\hat{\Omega}_S^{(k)}$ and $\hat{\Omega}_S^{(j)}$ intersect the global boundary *S*, the domain $A^{k,j}$ is illustrated in Fig 4(a). Adopting the same technique applied for the evaluation of the boundary integrals $\mathbf{H}^{k,j}$, the numerical evaluation of the volume integral $\mathbf{D}^{k,j}$ defined on the domain $A^{k,j}$ is accomplished by splitting the integration domain $A^{k,j}$ into small triangular segments (Fig. 4(b)) and performing, for each segment separately, the integration in a local coordinate system ξ_1, ξ_2 through standard Gaussian quadrature. In the present work, the advanced Delaunay type triangular mesh generation algorithm, proposed recently by [Shewchuk (2002)], is employed for the splitting of $A^{k,j}$ into triangular segments.

5 Examples

In order to demonstrate the accuracy of the LBIE method presented in the previous sections three representative harmonic elastic problems are solved. In all the numerical examples presented in this section the boundary conditions have been taken into account with the aid of the simple transformation method of [Atluri, Kim, and Cho (1999)] and the direct procedure of [Gosz and Liu (1996)], both explained in paragraph 4.2. The main conclusion here is that both procedures provide results of the same accuracy with the later, however, being much more efficient than the first one. The first problem deals with the uniform harmonic tension of the plane 6m x 6m domain shown in Fig 5(a). The material properties are considered $E = 2.50E+06\ N/m^2$, $\nu = 0.25$ and $\rho = 100kg/m^3$ with E, ν, ρ denoting the Young modulus, the Poisson ration and the mass density, respectively. The prescribed boundary conditions are: zero shear traction along the four sides, zero displacements at the three supported sides and a normal, harmonic and uniform traction $t = 100N/m^2$ at the free side of the square. The first two resonance frequencies of the above described problem are $\omega_1 = 45.345, \omega_2 = 136.035$ [Dominguez (1993)]. For the LBIE method solution of the problem in the frequency rage 4 to 140 Hz, 81 ordered nodal points are used (Fig 5(b)). The radii of the support domains was selected to be the same for all nodes and equal to 1.55. The problem is solved with the aid of both methodologies addressed in the present work, i.e. the LBIE method and the LB/VIE method. The displacement and traction vectors at the nodes 1 and 2, respectively, are calculated and demonstrated in Figs 6 and 7. The obtained results are compared to the numerical ones taken with a BEM code reported in [Polyzos, Tsinopoulos, and Beskos (1998)]. Observing the results shown in Figs 6 and 7, one can say that (a) the agreement between LBIE method and BEM solutions is excellent and (b) for the same distribution of nodes both LBIE method and LB/VIE method provide results of the same accuracy. Next, consider a long cylindrical shell of density ρ, with inner and outer radii *a* and *b*, respectively, subjected to an internal uniform harmonic pressure $P(\omega) = P_i e^{i\omega t}$. The analytical expressions for displacements and tractions of this problem are given in the work of [Polyzos, Tsinopoulos, and Beskos (1998)] As in the previous example, this problem is solved numerically ($P_i = 1, \mu = 240, \nu = 0.25, \rho = 1, a = 0.8, b = 1.0$) with both the LBIE method and the

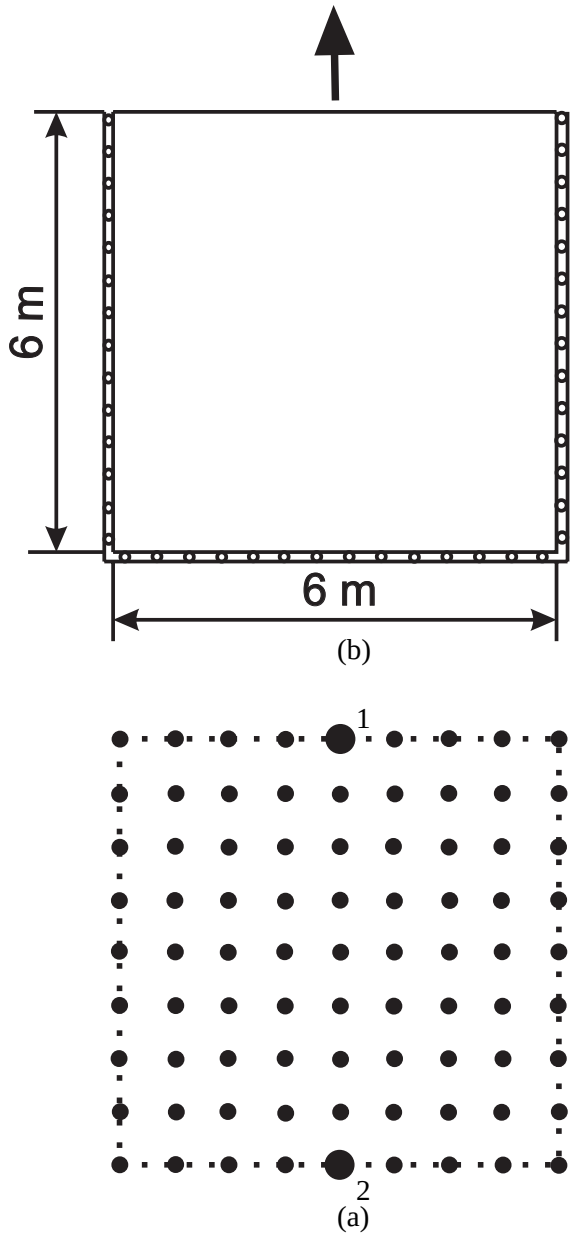

Figure 5 : (a) Tension of a square plane with a harmonic traction. (b) Distribution of the used nodal points

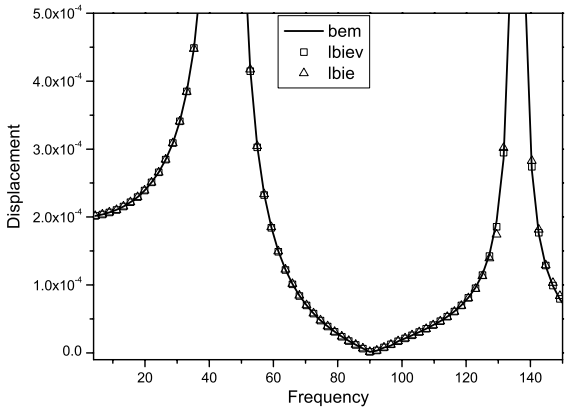

Figure 6 : Displacement at nodal point 1 versus frequency

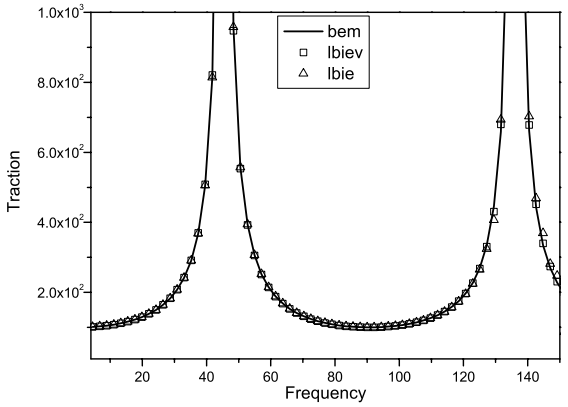

Figure 7 : Traction at nodal point 2 versus frequency

LB/VIE method. Due to the symmetry only one quarter of the problem needs to be considered (Fig 8(a)). For the solution of the problem in the frequency range of 1 to 440 rad/sec, a distribution of 877 nodes is employed for all the frequencies (Fig. 8(b)). In order to have a comparison between the LBIE method and the LB/VIE method, the same distribution of nodes are used for both methodologies. The radial displacement of node 1 as well as the shear traction vector at the node 2, shown in Fig. 8(b), are numerically evaluated and depicted in Figs 9 and 10, respectively. As it is evident, the numerical results obtained by the proposed here LBIE method and LB/VIE method are in excellent agreement with the analytical ones. Also, as in the previous example, it should be noticed that for the same distribution of nodes both LBIE method and LB/VIE method provide results of the same accuracy.

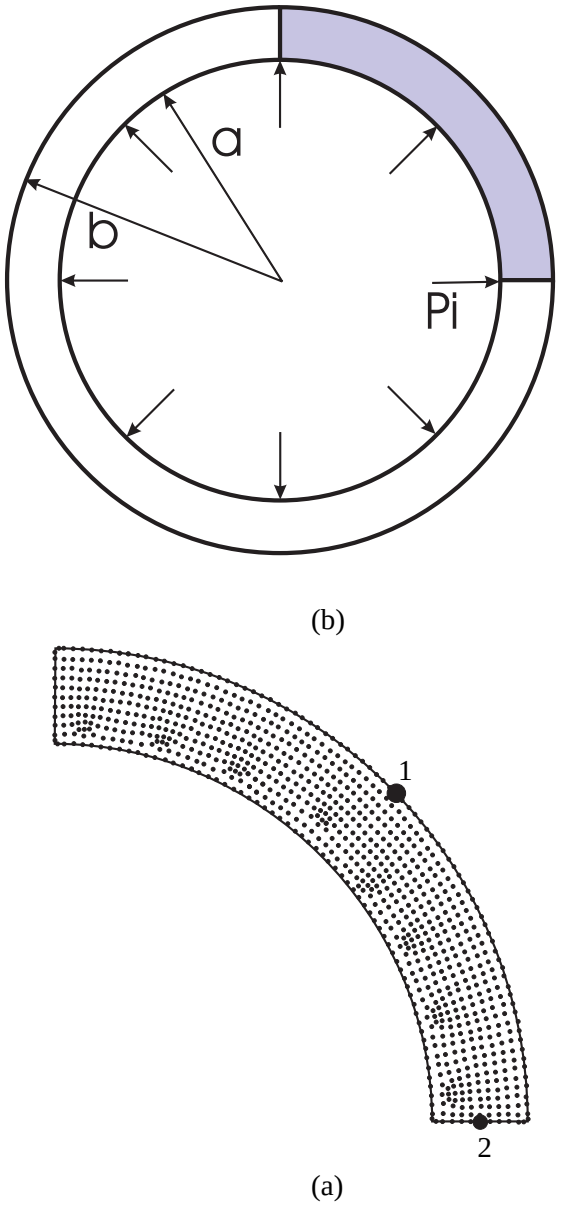

Figure 8 : (a) Hollow cylinder subjected to internal pressure P_i. (b) Distribution of the used nodal points at the one quarter of the cylinder.

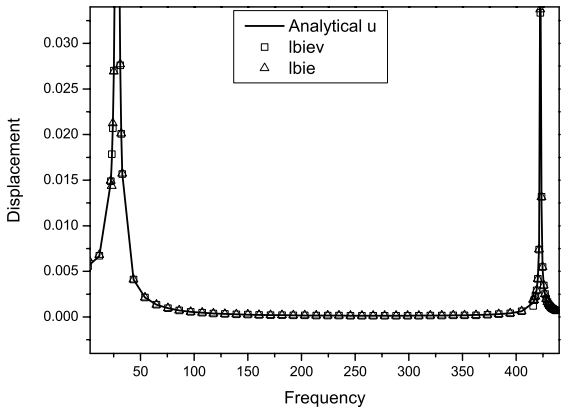

Figure 9 : Displacement at nodal point 1 versus frequency

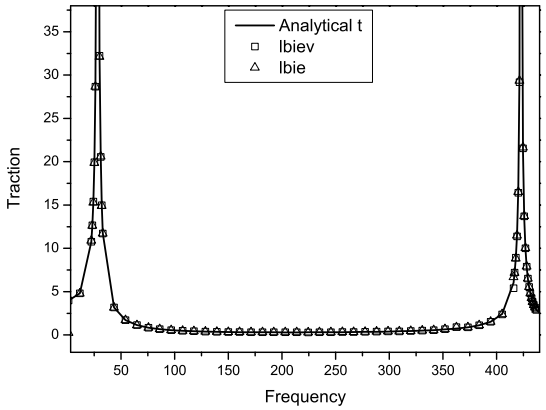

Figure 10 : Traction at nodal point 2 versus frequency

The third example deals with the harmonic excitation of the cantilever beam of Fig 11. The problem is solved for plane strain conditions with $P = 1, E = 1, D = 1, L = 8$ and $\nu = 0.25$. Both LBIE method and LB/VIE method

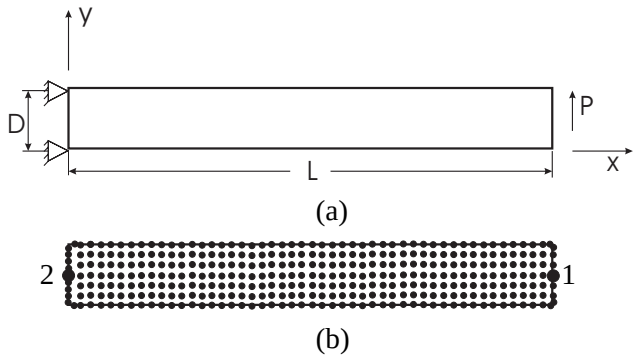

Figure 11 : (a) Bending of a cantilever beam. (b) Distribution of the used nodal points.

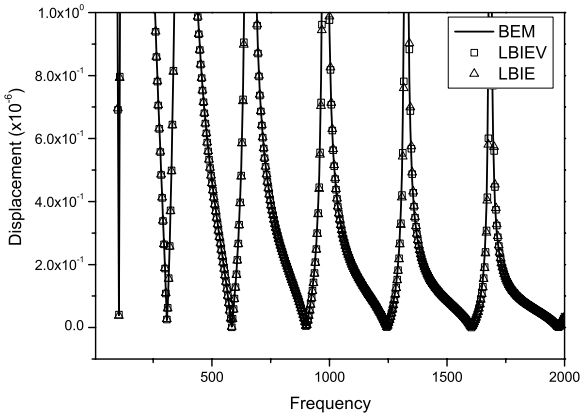

Figure 12 : Displacement at nodal point 1 versus frequency

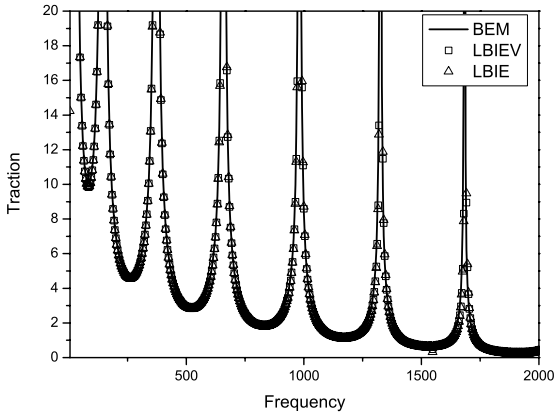

Figure 13 : Traction at nodal point 2 versus frequency

are employed and the vertical displacement as well as the normal tractions at the points 1 and 2 respectively are evaluated. A uniform distribution of 349 nodal points is used and the radii of the support domains are selected to be the same for all nodes and equal to 0.384. The obtained results are depicted in Fiqs 12 and 13 and compared to the corresponding ones taken with the BEM code described in Polyzos et. al (1998). As it is evident the agreement is very good for both LBIE method and LB/VIE method.

6 Conclusions

Two new meshless local integral equation methods for solving two dimensional frequency domain elastodynamic problems have been proposed. The first, called local boundary integral equation (LBIE) method, utilizes the frequency domain elastodynamic fundamental solution, thus concluding to a boundary only local integral formulation, while the second one, called local boundary/volume integral equation (LB/VIE) method, makes use of the static fundamental solution, which derives both surface and volume integrals in the final local integral representation of displacements. In order to get rid of tractions on the local boundaries, the LBIE and the LB/VIE methods exploit the elastodynamic and the elastostatic companion solutions, respectively, with the first derived explicitly in the framework of the present paper. The interpolation of the internal and boundary vector fields is accomplished with the aid of the moving least squares (MLS) approximation. On the global boundary displacements and tractions are treated as independent variables. Thus, derivatives of the MLS interpolation shape functions are avoided throughout the numerical implementation of the two methods. The transformation method of [Atluri, Kim, and Cho (1999)] as well as the direct procedure of [Gosz and Liu (1996)] , both explained in the paragraph 4.2, have been used for the enforcement of the essential boundary conditions. The surface and volume integrals defined over the support domain of each node have been evaluated with great accuracy by means of some very efficient numerical techniques described in the paragraph 4.3. Highly accurate and direct integration techniques proposed by Guiggiani and co- workers have been employed for the numerical evaluation of the singular integrals appearing in both

LBIE and LB/VIE methods formulations. Three representative plane strain elastodynamic problems have been solved in order to demonstrate the high accuracy of the proposed methodologies. On the basis of the obtained results, the following two interesting conclusions can be drawn:

1.For the same distribution of nodes both the LBIE and the LB/VIE methods provide solutions of the same accuracy. This fact indicates the versatility of the LB/VIEM since it can be successfully used for the solution of anisotropic, non- homogeneous and non-linear elastodynamic problems where the corresponding fundamental solutions are not available.

2. Comparing the results taken by the LB/VIE method when the essential boundary conditions are imposed through the transformation method of [Atluri, Kim, and Cho (1999)] with those taken when the direct procedure of [Gosz and Liu (1996)] is employed for the enforcement of the boundary conditions, one can say that both methodologies provide results of the same accuracy with the later being much more efficient than the first one.

Acknowledgement: The authors acknowledge with thanks the support of the Greek Institute of Governmental Scholarships (I.K.Y) through the program IKYDA 2002 (Scientific cooperation between the University of Patras, Greece and the Ruhr- University Bochum, Germany).

References

Atluri, S. N.; Kim, H.-G.; Cho, J. Y. (1999): A critical assessment of the truly Meshless Local Petrov-Galerkin (MLPG) and Local Boundary Integral Equation (LBIE) methods. *Comp. Mech.*, vol. 24, pp. 348–372.

Atluri, S. N.; Shen, S. P. (2002): *The Meshless Local Petrov-Galerkin (MLPG) Method*. Tech Science Press.

Atluri, S. N.; Shen, S. P. (2002): The meshless local Petrov-Galerkin (MLPG) method: A simple and less costly alternative to the finite element and boundary element methods. *CMES: Computer Modeling in Engineering & Sciences*, vol. 3, pp. 11–51.

Atluri, S. N.; Sladek, J.; Sladek, V.; Zhu, T. (2000): The local boundary integral equation (LBIE) and it's meshless implementation for linear elasticity. *Comp. Mech.*, vol. 25, pp. 180–198.

Atluri, S. N.; Zhu, T. (1998): A New Meshless Local Petrov-Galerkin (MLPG) Approach in Computational Mechanics. *Computational Mechanics*, vol. 22, pp. 117–127.

Atluri, S. N.; Zhu, T. (2000): New concepts in meshless methods. *Int. J. Numer. Methods Engng.*, vol. 47, pp. 537–556.

Belytchko, T.; Krongauz, Y.; Organ, D.; Fleming, M. (1996): Meshless methods: an overview and recent developments. *Comp. Meth. Appl. Mech. Engng.*, vol. 139, pp. 3–47.

Beskos, D. E. (1987): Boundary element methods in dynamic analysis. *Appl. Mech.*, vol. 40, pp. 1–23.

Beskos, D. E. (1997): Boundary element methods in dynamic analysis. Part II. *Appl. Mech.*, vol. 50, pp. 149–197.

Brebbia, C. A.; Dominguez, J. (1989): *Boundary Elements. An Introductory Course*. Computational Mechanics Publications, Southampton.

Breitkopf, P.; Rassineux, A.; Touzot, G.; Villon, P. (2000): Explicit form and efficient computation of MLS shape functions and their derivatives. *Int. J. Numer. Meth. Engng.*, vol. 48, pp. 451–466.

Chen, J. S.; Pan, C.; Wu, C. T.; Liu, W. K. (1996): Reproducing kernel methods for large deformation analysis on nonlinear structures. *Comput. Mathods Appl. Mech. Eng.*, vol. 139, pp. 195–227.

Dassios, G.; Lindell, I. V. (2001): On the helmholtz decomposition for polyadics. *Quarterly of Appl. Math.*, vol. LIX4, pp. 787–796.

Dominguez, J. (1993): *Boundary Elements in Dynamics*. CMP, Southampton and Elsevier Applied Sience, London.

Gosz, S.; Liu, W. K. (1996): Admissible approximations for essential boundary conditions in the reproducing kernel particle method. *Comp. Mech.*, vol. 19, pp. 120–135.

Guiggiani, M.; Casalini, P. (1987): Direct computation of Cauchy principal value integrals in advanced boundary elements. *Int. J. Numer. Methods Engng.*, vol. 24, pp. 1711–1720.

Gunther, F.; Liu, W. K. (1998): Implementation of boundary conditions for meshless methods. *Comput. Mathods Appl. Mech. Eng.*, vol. 163, pp. 205–230.

Kogl, M.; Gaul, L. (2000): A 3-D Boundary Element Method for Dynamic Analysis of Anisotropic Elastic Solids. *CMES: Computer Modeling in Engineering & Sciences*, vol. 1, pp. 27–44.

Lancaster, P.; Salkauskas, K. (1981): Surface generation by moving least square methods. *Math. Comput.*, vol. 37, pp. 141–158.

Li, S.; Liu, W. K. (2002): Meshfree and particle methods and their applications. *Appl. Mech. Rev.*, vol. 54, pp. 1–34.

Long, S.; Zhang, Q. (2002): Analysis of thin plates by the local boundary integral equation (LBIE) method. *Engng. Anal. Boundary Elem.*, vol. 26, pp. 707–718.

Manolis, G. D.; Beskos, D. E. (1988): *Boundary Element Methods in Elastodynamics*. Unwin Hyman, London.

Manolis, G. D.; Pavlou, S. (2000): A Green's Function for Variable Density Elastodynamics under Strain Conditions by Hormander's Method. *CMES: Computer Modeling in Engineering & Sciences*, vol. 3, pp. 399–416.

Polyzos, D.; Tsinopoulos, S. V.; Beskos, D. E. (1998): Static and dynamic boundary element analysis in incompressible linear elasticity. *European. J. Mech. A/Solids*, vol. 17, pp. 515–536.

Shewchuk, J. R. (2002): Delaunay refinement algorithms for triangular mesh generation. *Computational Geometry*, vol. 22, pp. 21–74.

Sladek, J.; Sladek, V. (2002): A Trefftz function approximation in local boundary integral equations. *Comp. Mech.*, vol. 28, pp. 212–219.

Sladek, J.; Sladek, V. (2003): Application of local boundary integral method in to micropolar elasticity. *Engng. Anal. Boundary Elem.*, vol. 27, pp. 81–90.

Sladek, J.; Sladek, V.; Atluri, S. N. (2000): Local boundary integral equation (LBIE) method for solving problems of elasticity with nonhomogeneous material properties. *Comp. Mech.*, vol. 24, pp. 456–462.

Sladek, J.; Sladek, V.; Atluri, S. N. (2001): A pure contour formulation for meshless local boundar integral equation method in thermoelasticity. *CMES: Computer Modeling in Engineering & Sciences*, vol. 2, pp. 423–434.

Sladek, J.; Sladek, V.; Keer, R. V. (2002): New integral equation approach to solution of diffusion equation. *Comp. Assisted Mech. and Engng. Sci.*, vol. 9, pp. 555–572.

Sladek, J.; Sladek, V.; Keer, R. V. (2003): Meshless local boundary integral equation method for 2D elastodynamic problems. *Int. J. Numer. Meth. Engng.*, vol. 57, pp. 235–249.

Sladek, J.; Sladek, V.; Mang, H. A. (2002): Meshless formulation for simply supported and clamped plate problems. *Int. J. Numer. Meth. Engng.*, vol. 55, pp. 359–375.

Sladek, J.; Sladek, V.; Mang, H. A. (2002): Meshless local boundary integral equation method for plates resting on elastic foundation. *Comput. Meth. Appl. Mech. Eng.*, vol. 191, pp. 5943–5959.

Sladek, J.; Sladek, V.; Mang, H. A. (2003): Meshless LBIE formulationsfor simply supported and clamped plates under dynamic load. *Computers and Structures*, vol. 81, pp. 1643–1651.

Sladek, V.; Sladek, J.; Atluri, S. N. (2002): Application of the local boundary integral equation method to boundary value problems. *Int. Appl. Mech.*, vol. 38, pp. 1025–1043.

Sladek, V.; Sladek, J.; Atluri, S. N.; Keer, R. V. (2000): Numerical integration of singularities of local boundary integral equations. *Comp. Mech.*, vol. 25, pp. 394–403.

Wagner, G. J.; Liu, W. K. (2000): Application of essential boundary conditions in mesh-free methods: A corrected collocation method. *Int. J. Numer. Meth. Engng.*, vol. 47, pp. 1367–1379.

Zhu, T. (1999): A new meshless regular local boundary integral equation (MRLBIE) approach. *Int. J. Numer. Methods Engng.*, vol. 46, pp. 1237–1252.

Zhu, T.; Zhang, J. D.; Atluri, S. N. (1998): A local boundary integral equation (LBIE) method in computational mechanics and a meshless discretization approach. *Comp. Mech.*, vol. 21, pp. 223–235.

Zhu, T.; Zhang, J. D.; Atluri, S. N. (1998): A meshless local boundary integral equation (LBIE) for solving nonlinear problems. *Comp. Mech.*, vol. 22, pp. 174–186.

Zhu, T.; Zhang, J. D.; Atluri, S. N. (1999): A meshless numerical method based on the local boundary integral equation (LBIE) to solve linear and non-linear boundary value problems. *Engng. Anal. Boundary Elem.*, vol. 23, pp. 375–389.

Appendix A: 2D companion solutions

In this appendix the elastostatic and frequency domain elastodynamic companion solutions $\mathbf{U}^c$ and $\mathbf{u}^c$, respectively, are explicitly derived. Allthough the elastostatic companion solution in known from the literature, it is derived here just for illustration purposes.

Appendix A:.1 2d Elastostatic companion solution

According to Eq. 13 the 2D elastostatic companion solution $\mathbf{U}^c$ satisfies the following boundary value problem

$$\begin{aligned} \mu\nabla^2\mathbf{U}^c(r)+(\lambda+\mu)\nabla\nabla\cdot\mathbf{U}^c(r)=\mathbf{0}, r\le r_0 \\ \mathbf{U}^c(r_0)=\mathbf{U}^*(r_0) \end{aligned} \tag{48}$$

where $\mathbf{U}^*(r)$ is the 2D elastostatic fundamental solution having the form [Brebbia and Dominguez (1989)]

$$\mathbf{U}^*=\frac{1}{8\pi\mu(1-\nu)}[(4\nu-3)\ln r\tilde{\mathbf{I}}+\hat{\mathbf{r}}\otimes\hat{\mathbf{r}}] \tag{49}$$

Applying the Helmholtz decomposition theorem proposed by [Dassios and Lindell (2001)], $\mathbf{U}^c$ can be written as

$$\mathbf{U}^c(r)=\nabla\nabla\phi(r)+\nabla\nabla\times\mathbf{A}(r)+\nabla\times\nabla\times\mathbf{G}(r) \tag{50}$$

where $\phi(r)$ is a scalar function, $\mathbf{A}(r)$ a vector function and $\mathbf{G}(r)$ a dyadic function. Since $\phi(r)$, $\mathbf{A}(r)$ and $\mathbf{G}(r)$ are functions of r, it is easy to see one that

$$\nabla\times\mathbf{A}(r)=\mathbf{0} \tag{51}$$

and

$$\begin{aligned} \mathbf{0}=&\nabla\nabla\left(c_1r^2+c_2\right)+ \\ &\nabla\times\nabla\times\left[\left(2c_1r^2+c_2\right)\tilde{\mathbf{I}}+2c_1r^2\hat{\mathbf{r}}\otimes\hat{\mathbf{r}}\right] \end{aligned} \tag{52}$$

where c_1, c_2 are constants. Substituting Eqs (50) and (52) into the first equation of (48) and taking into account Eq. (51) and the identities

$$\begin{aligned} \nabla^2\nabla\nabla\phi&=\nabla\nabla\nabla^2\phi \\ \nabla^2\left(\nabla\times\nabla\times\mathbf{G}\right)&=\nabla\times\nabla\times\left(\nabla^2\mathbf{G}\right) \end{aligned} \tag{53}$$

one obtains

$$\begin{aligned} &\nabla\nabla\left[\frac{2\mu(1-\nu)}{1-2\nu}\nabla^2\phi\right]+\nabla\times\nabla\times\left(\mu\nabla^2\mathbf{G}\right)= \\ &\nabla\nabla\left(c_1r^2+c_2\right)+ \\ &\nabla\times\nabla\times\left[\left(2c_1r^2+c_2\right)\tilde{\mathbf{I}}+2c_1r^2\hat{\mathbf{r}}\times\hat{\mathbf{r}}\right] \end{aligned} \tag{54}$$

Due to the irrotational and solenoidal nature of $\phi(r)$ and $\mathbf{G}(r)$ respectively, Eq. (54) is satisfied when

$$\nabla^2\phi=\frac{1-2\nu}{2\mu(1-\nu)}\left(c_1r^2+c_2\right) \tag{55}$$

$$\nabla^2\mathbf{G}=\frac{1}{\mu}\left(2c_1r^2+c_2\right)\tilde{\mathbf{I}}+\frac{2c_1}{\mu}r^2\hat{\mathbf{r}}\otimes\hat{\mathbf{r}} \tag{56}$$

Since $\mathbf{G}$ is a function of r it can be written as

$$\mathbf{G}(r)=G_1(r)\tilde{\mathbf{I}}+G_2(r)\hat{\mathbf{r}}\otimes\hat{\mathbf{r}} \tag{57}$$

Thus the scalar functions $\phi(r), G_1(r)$ and $G_2(r)$ satisfy the differential equations

$$\begin{aligned} &\frac{d^2\phi}{dr^2}+\frac{1}{r}\frac{d\phi}{dr}=\frac{1-2\nu}{2\mu(1-\nu)}\left(c_1r^2+c_2\right) \\ &\frac{d^2G_1}{dr^2}+\frac{1}{r}\frac{dG_1}{dr}+\frac{2G_2}{r^2}=\frac{1}{\mu}\left(2c_1r^2+c_2\right) \\ &\frac{d^2G_2}{dr^2}+\frac{1}{r}\frac{dG_2}{dr}-\frac{4G_2}{r^2}=\frac{2G_1}{\mu}r^2 \end{aligned} \tag{58}$$

and they have the form

$$\begin{aligned} \phi(r)&=\frac{1-2\nu}{8\mu(1-\nu)}\left(\frac{c_1}{4}r^4+c_2r^2\right) \\ G_1(r)&=\frac{5c_1}{48\mu}r^4-\frac{c_2}{4\mu}r^2 \\ G_2(r)&=\frac{c_1}{6\mu}r^4+\frac{c_2}{\mu}r^2 \end{aligned} \tag{59}$$

Inserting Eq. (59) into Eq. (50) and taking into account Eqs. (51) and (57) one eventually obtains

$$\begin{aligned} \mathbf{U}^c(r)=&\frac{3-4\nu}{4\mu(1-\nu)}c_1r^2\hat{\mathbf{r}}\otimes\hat{\mathbf{r}}-\frac{5-4\nu}{8\mu(1-\nu)}c_1r^2\tilde{\mathbf{I}}+ \\ &\frac{4-5\nu}{4\mu(1-\nu)}c_2\tilde{\mathbf{I}} \end{aligned} \tag{60}$$

Satisfying the boundary conditions of the problem $\mathbf{U}^c(r_0)=\mathbf{U}^*(r_0)$, the constants c_1 and c_2 are easily evaluated and the elastostatic companion solution $\mathbf{U}^c(r)$ obtains the final form

$$\begin{aligned} \mathbf{U}^c(r)=&\frac{1}{8\pi\mu(1-\nu)}\frac{r^2}{r_0^2}\hat{\mathbf{r}}\otimes\hat{\mathbf{r}}+ \\ &\frac{1}{8\pi\mu(1-\nu)}\left[\frac{5-4\nu}{2(3-4\nu)}\left(1-\frac{r^2}{r_0^2}\right)+(4\nu-3)\ln r_0\right]\tilde{\mathbf{I}} \end{aligned} \tag{61}$$

Appendix A:.2 2D frequency domain elastodynamic companion solution

In the present case, as companion solution is defined the tensor $\mathbf{u}^c(r)$ that satisfies the following boundary value problem

$$\mu\nabla^2\mathbf{u}^c(r)+(\lambda+\mu)\nabla\nabla\cdot\mathbf{u}^c(r)+\rho\omega^2\mathbf{u}^c(r)=\mathbf{0}, r\le r_0$$
$$\mathbf{u}^c(r_0)=\mathbf{u}^*(r_0) \tag{62}$$

where $\mathbf{u}(r)$ is the 2D frequency domain elastodynamic fundamental solution written as [Dominguez (1993)]

$$\begin{aligned}\mathbf{u}^*(r)&=\frac{1}{2\pi\mu}\left(\Psi(r)\tilde{\mathbf{I}}-X(r)\hat{\mathbf{r}}\otimes\hat{\mathbf{r}}\right)\\ \Psi(r)&=K_0(ik_sr)+\frac{1}{ik_sr}\left[K_1(ik_sr)-\frac{C_s}{C_p}K_1(ik_pr)\right]\\ X(r)&=K_2(ik_sr)-\frac{C_s^2}{C_p^2}K_2(ik_pr)\end{aligned} \tag{63}$$

where $K_n(a)$ is the second kind modified Bessel function of order n, k and c represent wave numbers and wave phase velocities, respectively, and the subscripts p and s indicate longitudinal and shear wave respectively. Considering the Helmholtz decomposition form of Eq. 50 for $\mathbf{u}(r)$ and applying the same procedure as in the static case, one concludes to the following system of differential equations, which should be satisfied by the scalar functions $\phi(r)$, $G_1(r)$ and $G_2(r)$

$$\begin{aligned}&\frac{d^2\phi}{dr^2}+\frac{1}{r}\frac{d\phi}{dr}+{k_p}^2\phi=\frac{1-2\nu}{2\mu(1-\nu)}\left(c_1r^2+c_2\right)\\ &\frac{d^2G_1}{dr^2}+\frac{1}{r}\frac{dG_1}{dr}+{k_s}^2G_1+\frac{2G_2}{r^2}=\frac{1}{\mu}\left(2c_1r^2+c_2\right)\\ &\frac{d^2G_2}{dr^2}+\frac{1}{r}\frac{dG_2}{dr}+{k_s}^2G_2-\frac{4G_2}{r^2}=\frac{2c_1}{\mu}r^2\end{aligned} \tag{64}$$

Since only the dynamic behavior of $\mathbf{u}^c$ is considered the constants c_1 and c_2 are taken to be equal to zero. Thus the system (64) obtains the form

$$\begin{aligned}&z^2\frac{d^2\phi^2}{dz^2}+z\frac{d\phi}{dz}-z^2\phi=0\\ &\zeta^2\frac{d^2G_2}{d\zeta^2}+\zeta\frac{dG_2}{d\zeta}-\left(\zeta^2+4\right)G_2=0\\ &\zeta^2\frac{d^2G_1}{d\zeta^2}+\zeta\frac{dG_1}{d\zeta}-\zeta^2G_1=-2G_2\end{aligned} \tag{65}$$

where $z=ik_pr$ and $\zeta=ik_sr$ It is easy to find one that the solution of system (65) is

$$\begin{aligned}\phi(r)&=D_1I_0(ik_pr)\\ G_1(r)&=D_3I_0(ik_sr)-\frac{D_2}{2}I_2(ik_sr)\\ G_2(r)&=D_2I_2(ik_sr)\end{aligned} \tag{66}$$

where $I_n(a)$ is the first kind modified Bessel functions of order n. Inserting Eq. (65) into Eq. 50 and taking in to account Eqs. 51 and 57 one takes

$$\begin{aligned}\mathbf{u}^*(r)=&\left(\frac{d^2\phi}{dr^2}-\frac{1}{r}\frac{d\phi}{dr}\right)\hat{\mathbf{r}}\otimes\hat{\mathbf{r}}+\frac{1}{r}\frac{d\phi}{dr}\tilde{\mathbf{I}}+\\ &\left(\frac{d^2G_1}{dr^2}-\frac{1}{r}\frac{dG_1}{dr}\right)\hat{\mathbf{r}}\otimes\hat{\mathbf{r}}-\frac{d^2G_1}{dr^2}\tilde{\mathbf{I}}+\\ &\left(2\frac{G_2}{r_2}-\frac{1}{r}\frac{dG_2}{dr}\right)\hat{\mathbf{r}}\otimes\hat{\mathbf{r}}+\left(\frac{1}{r}\frac{dG_2}{dr}-\frac{G_2}{r^2}\right)\tilde{\mathbf{I}}\end{aligned} \tag{67}$$

After some algebra, one can find that

$$\frac{d^2\phi}{dr^2}-\frac{1}{r}\frac{d\phi}{dr}=-D_1k_p^2I_2(ik_pr) \tag{68}$$

$$\frac{1}{r}\frac{d\phi}{dr}=\frac{D_1}{2}k_p^2\left[I_2(ik_pr)-I_0(ik_pr)\right] \tag{69}$$

$$\begin{aligned}&\frac{d^2G_1}{dr^2}-\frac{1}{r}\frac{dG_1}{dr}+\frac{2G_2}{r^2}-\frac{1}{r}\frac{dG_2}{dr}=\\ &-k_s^2\left(D_3-\frac{D_2}{2}\right)I_2(ik_sr)\end{aligned} \tag{70}$$

$$\begin{aligned}&-\frac{d^2G_1}{dr^2}+\frac{1}{r}\frac{dG_2}{dr}-\frac{G_2}{r^2}=\\ &\frac{k_s^2}{r}\left(D_3-\frac{D_2}{2}\right)\left[I_0(ik_sr)+I_2(ik_sr)\right]\end{aligned} \tag{71}$$

Substituting the above relations to Eq. 67, one eventually obtains

$$\mathbf{U}(r)=\frac{1}{2\pi\mu}\left[\Psi(r)\tilde{\mathbf{I}}+\mathbf{X}(r)\hat{\mathbf{r}}\otimes\hat{\mathbf{r}}\right] \tag{72}$$

where

$$\begin{aligned}\Psi(r)=2\pi\mu\Bigg\{&\frac{D}{2}k_p^2\left[I_2(ik_pr)-I_0(ik_pr)\right]+\\ &\frac{R}{2}ks^2\left[I_2(ik_sr)+I_0(ik_sr)\right]\Bigg\}\end{aligned} \tag{73}$$

and

$$X(r) = -2\pi\mu\left[Dk_p^2 I_2(ik_p r) + Rk_s^2 I_2(ik_s r)\right] \tag{74}$$

The constants D and $R = D_3 - \frac{D_2}{2}$ can be evaluated with the aid of the boundary condition $\mathbf{u}^c(r) = \mathbf{u}^*(r)$. Thus, satisfying the second equation of (62) the constants D and R are found to be

$$\begin{aligned} D &= \frac{P\left[I_2(s) + I_0(s)\right] - QI_2(s)}{k_p^2\left[I_2(p)I_0(s) + I_2(s)I_0(p)\right]} \\ R &= \frac{QI_2(p) - P\left[I_2(p) - I_0(p)\right]}{k_s^2\left[I_2(p)I_0(s) + I_2(s)I_0(p)\right]} \end{aligned} \tag{75}$$

where

$$\begin{aligned} &p = ik_p r_0\ ,\ s = ik_s r_0 \\ &P = \frac{1}{2\pi\rho C_s^2}\left[K_2(s) - \frac{C_s^2}{C_p^2}K_2(p)\right] \\ &Q = \frac{1}{\pi\rho C_s^2}\left[K_0(s) + \frac{1}{ik_s r_0}\left[K_1(s) - \frac{C_s}{C_p}K_1(p)\right]\right] \end{aligned} \tag{76}$$